JOURNAL OF CATALYSIS 108, 383–400 (1987)

Study of the Morphology and Structure of Niobia–Silica Surface Oxides Using Model Thin Films

J. G. WEISSMAN,* E. I. KO,* AND P. WYNBLATT†

*Department of Chemical Engineering and †Department of Metallurgical Engineering and Materials Science, Carnegie Mellon University, Pittsburgh, Pennsylvania 15213

Received March 23, 1987; revised July 14, 1987

Model thin films of niobia 4, 12, and 50 Å thick, corresponding to 1, 3, and 13 monolayers, deposited by RF-sputtering onto silica (Nb_2O_5–SiO_2), were prepared for a study of the interactions between surface and supporting oxides. These samples were treated in air at 773 and 873 K for up to 16 h and then observed by electron microscopy. For reactively sputtered films, Nb_2O_5 in monolayer and multilayer amounts dewetted the substrate after heating at 773 K, and crystallized to either T- and/or H-Nb_2O_5 at 873 K. These observations are different from those found for Nb_2O_5–SiO_2 high-surface-area samples, prepared by incipient wetness impregnation and similarly treated. In the high-surface-area samples, there is a strong interaction which results in the stabilization of surface-phase Nb_2O_5 at a monolayer coverage and formation of T-Nb_2O_5 at higher loadings. The difference in behavior between the low- and high-surface-area samples can be understood in terms of stabilization of surface niobia due to surface hydroxyl groups in the latter. These results illustrate the applicability of model thin films to the study of surface oxides.

INTRODUCTION

A *surface-phase oxide* is defined in this paper as a material consisting of one oxide stabilized and dispersed on the surface of a different oxide to a monolayer coverage or less. The term *surface oxide* is used to denote a system in which the supported phase has a larger than monolayer coverage or is weakly interactive with the underlying oxide. The surface structure, surface chemistry, and catalytic behavior of surface-phase and surface oxides have been extensively studied by numerous workers (*1–14*). Common examples are V_2O_5/TiO_2 oxidation catalysts and MoO_3/Al_2O_3 hydrodesulfurization catalysts.

A theme common to these studies has been the effects of changing variables such as support phase and composition, preparation temperature and environment, and surface oxide loading on the catalytic properties of the systems studied. Although much has been learned concerning the chemical nature of surface oxides, including the type of bonding, both within the surface oxides and to substrates, and the valence of surface species, comparatively little work has appeared on the physical structure of the surface phase and the role of the underlying support on the surface structure.

V_2O_5 surface oxide catalysts serve as a good example of how the support can strongly influence the structure of surface oxides and, in turn, their catalytic properties. V_2O_5 interacts differently on different supports. On TiO_2, the (010) face of V_2O_5 is selectively exposed (*1–3*), leading to high activity for reactions such as *o*-xylene oxidation and to high surface acidity, as compared to V_2O_5 supported on Al_2O_3 or SiO_2, where no preferred crystal orientation to the surface was found (*4–6*). Others have also found that the composition of the support strongly affects the structure of the supported V_2O_5 over many support compositions (*7, 8*).

The structure of the support may influence the structure of the oxide on the surface. While Inomata *et al.* have reported

0021-9517/87 $3.00

that modifications of the TiO_2 support, either anatase, rutile, or both, have no effect on the overlying V_2O_5 structure (*3*), others have reported a support-phase effect, where anatase-supported V_2O_5 has a higher activity (*9*). The effects of different preparation methods could be responsible for these differences.

Observations similar to these have been reported for other systems. For MoO_3 supported on various oxides including Al_2O_3, TiO_2, CeO_2, and ZrO_2, different surface structures were found depending on the support (*10*). Del Arco *et al.* found that V_2O_5 and MoO_3 supported on TiO_2 had different structures; V_2O_5 occurred as patches on the support while MoO_3 was continuous (*11*). The effects of surface oxide loading on the structure have also been noted. Below a certain coverage, both WO_3 and MoO_3 on SiO_2 remains as stable surface-phase oxides, while above a certain coverage, distinct crystals were observed (*12, 13*). Similar behavior occurs in the V_2O_5/TiO_2 system (*14*).

These results clearly indicate the strong influence of the support on the structure, and thus the catalytic behavior, of surface oxides which can have varying extents of interaction with the substrate. Thus there is a need for better understanding this influence, especially where the support may also be a catalyst for some reactions. An example is the oxidation of methanol and n-heptanol over TiO_2, which is used as an oxide support (*7*). The selectivity of these reactions changes as a function of the support used and the extent of surface coverage, as any exposed support can exert influence on the products. A study of the "wettability" of the support by supported oxides may lead to new insights into the nature of these interactions and to the development of more advanced catalysts.

With this goal in mind, we undertook a study of niobia–silica (Nb_2O_5–SiO_2) surface oxides. This combination is effective as a catalyst in aldol condensation reactions (*15*), and has been extensively studied by Ko *et al.* as a support for metal catalysts (*16, 17*). Nickel was found to interact less strongly with a Nb_2O_5–SiO_2 surface-phase oxide than with bulk Nb_2O_5 under similar reduction conditions (*16*). These results suggested that the behavior of niobia on silica is crucial to the behavior of the surface-phase oxide toward nickel, with the key point being whether niobia wets, partially wets, or completely dewets the silica surface. In particular, the main interest is to define how the support/surface-phase interaction varies as a function of loading and/or the environment of the surface-phase oxide.

In order to observe directly the wetting behavior of Nb_2O_5 by transmission electron microscopy (TEM), we have prepared Nb_2O_5–SiO_2 model thin films by following a procedure similar to that used by Ruckenstein and others (*18–20*). Our preliminary results demonstrated that these topologically flat films are convenient and appropriate for TEM study (*21*). In this paper we report the effects of preparation conditions and treatment on the wettability and crystallization of Nb_2O_5 on SiO_2 in the model thin films and compare their behavior to the high-surface-area analogues.

EXPERIMENTAL

Preparation. Two series of niobia–silica (Nb_2O_5-SiO_2) surface oxide materials were prepared: high-surface-area (HSA) and thin film (TF). Details of the preparation procedure and characterization of the HSA samples have been reported elsewhere (*16*). In brief, a hexane solution of niobium(V) ethoxide (Alfa Products) were impregnated onto high-surface-area (300 m^2/g) silica (SiO_2, Davison grade 952) to incipient wetness. The niobia precursor was decomposed in nitrogen at 673 K for 2 h, and then calcined in oxygen at 773 K for 2 h. This procedure produced a homogeneous monolayer of niobia, and can be repeated to deposit subsequent second and third layers of Nb_2O_5.

Two types of TF samples were made,

one on silicon wafers suitable for surface analysis, and the other (the majority of the samples prepared) on silica thin films suitable for electron microscopy. In a method similar to that used by Schmidt *et al.* (*19*) and others (*20*), crushed silicon (Atomergic Chemicals Corp.) was placed in a tungsten boat held between copper electrodes inside a diffusion-pumped bell jar which has base pressure of about 1×10^{-6} torr. In order to produce flat, uniform films, the silicon was evaporated onto cleaved single-crystal halite surfaces, and the thickness as deposited was measured *in situ* with a quartz crystal thickness monitor. The films were then floated off of the halite and picked up onto 200-mesh stainless steel grids. These were then oxidized at 1273 K for 4 h in flowing air (3 liters/h) to produce amorphous silica films approximately 500–1000 Å thick. The other type of silica support was prepared by oxidizing both sides of a silicon (111) wafer (Atomergic Chemicals Corp.) as above, then stripping the oxide off of one surface with a few drops of 40% hydrofluoric acid to provide a conducting surface. This produced about 800 Å of silica supported by silicon.

Niobium was RF-sputter-deposited onto the silica TF supports. A conventional diode-type RF sputtering system was used, operating at 13.56 MHz and coupled to the cathode. The target was a foil of niobium (99.8%, Alfa Products) insulated from the cathode by an alumina supporting disk. Depositions were done using argon or oxygen/argon mixtures as the discharge gas, and as-deposited thicknesses were measured by a quartz crystal thickness monitor which had a resolution of about 2 Å for niobia. As-deposited thicknesses were estimated from the amount of mass needing to be coated on the quartz crystal surface to produce a measured change in the frequency of the crystal's vibration. Experimentally determined deposition rates were about 10 Å/min in Ar and 3 Å/min in O_2/Ar. Thicknesses equivalent to 4, 12, and 50 Å were prepared, corresponding to 1, 3, and 13 monolayers of Nb_2O_5, based on the volume coverage of a Nb_2O_5 monolayer on an HSA support (*16*). This procedure resulted in two series of samples, those that were inertly sputtered (IS) in argon and those that were reactively sputtered (RS) in oxygen/argon mixture.

After sputtering, the films were exposed to oxygen for a few minutes before removal from the sputtering chamber and exposure to atmosphere in order to minimize surface contamination. The as-deposited niobium TF's were oxidized at 773 and 873 K for 2, 6, and 16 h in flowing air (3 liters/h), similar to the treatment of the HSA samples (*16*).

Characterization. Surface analysis of the TF samples was affected by either X-ray photoelectron spectroscopy (XPS) performed at the University of Minnesota Surface Analysis Center or by scanning Auger microprobe (SAM). Both HSA and TF samples were examined by TEM on a JEOL JEM 120CX electron microscope. No additional preparation was necessary for TEM on the TF samples, while HSA samples were prepared by ultrasonically suspending a powdered sample in water, then placing a drop onto a holey carbon film supported on a copper grid and allowing the drop to dry.

RESULTS

Thin films. Silica thin films as prepared above were examined by TEM and a typical region is shown in Fig. 1. In general, the

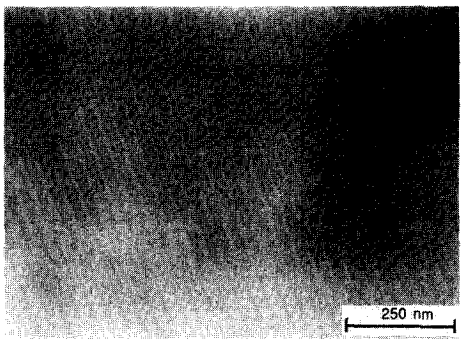

Fig. 1. TEM photomicrograph of 800-Å amorphous SiO_2 thin film, illustrating uniform contrast.

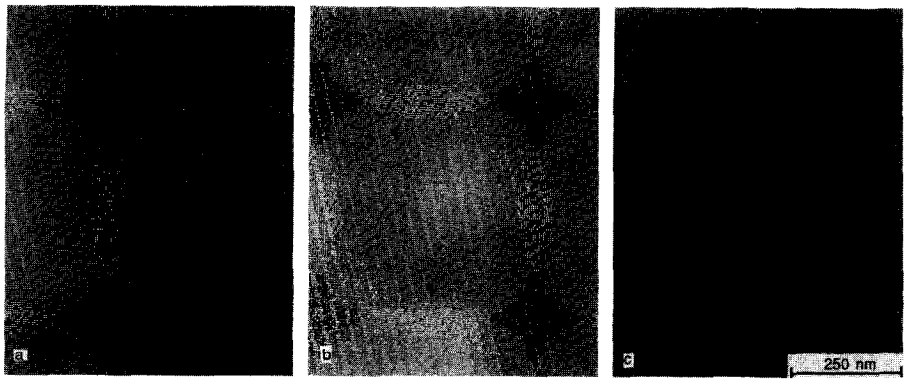

Fig. 2. TEM photomicrograph of inertly sputtered (IS) monolayer Nb_2O_5 film, showing development of dewetting with length of time of heating at 773 K. Some indistinct crystallites are visible in (c). The changes in overall contrast are due to different silica film thicknesses. (a) 4(—,A), (b) 4(500,2,A), (c) 4(500,16,A).

oxidized films have weak contrast features, indicating that they are amorphous and homogeneous. Occasionally, crystallites of tridymite, the medium-temperature phase of SiO_2, were observed and identified by comparing *d*-spacings obtained using transmission electron diffraction (TED) data with tabulated values (*22*). The presence of these crystals indicated that the films were fully oxidized. Surface analysis of the silica films indicated the presence of only Si and O, but with a small surface C contamination, as found by XPS and SAM.

As-deposited sputtered niobium films are depicted in Figs. 2a, 3a, and 4. Films deposited in an inert atmosphere, such as 50(—,A) (Fig. 4a),[1] exhibit a salt and pepper contrast found neither in micrographs of the reactively sputtered films, such as 50(—,O) (Fig. 4b), nor in the clean film (Fig. 1). This contrast difference was found

[1] The nomenclature 4(—,A) indicates a 4-Å film of Nb_2O_5, as deposited and inertly sputtered (IS) in argon; while 12(600,6,O) would indicate a 12-Å Nb_2O_5 film, heated at 873 K (600°C) for 6 h, made by reactive sputtering (RS) in oxygen/argon.

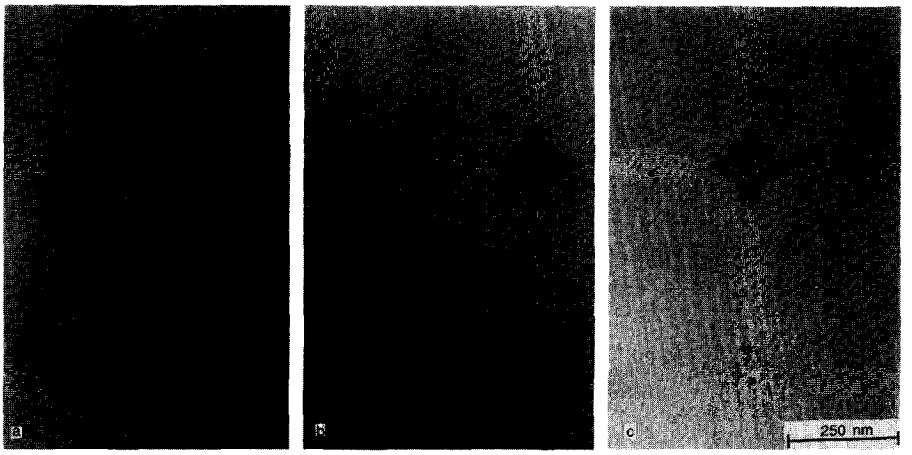

Fig. 3. TEM photomicrograph of reactively sputtered (RS) monolayer Nb_2O_5 films, showing development of dewetting, similar to, but not as extensive as that in Fig. 2. (a) 4(—,O), (b) 4(500,2,O), (c) 4(500,16,O).

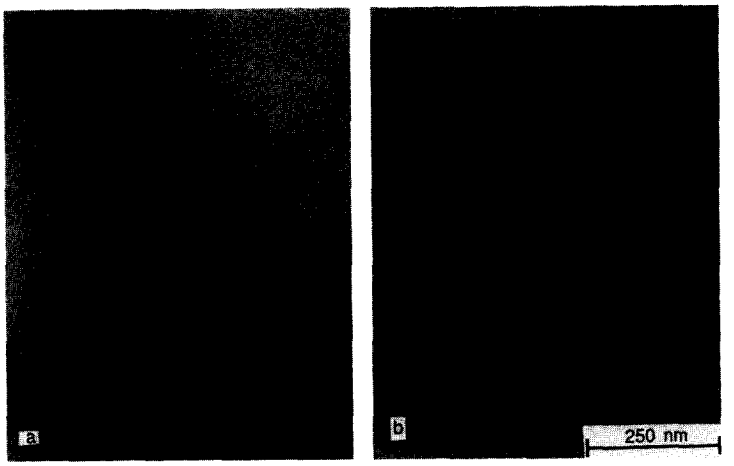

Fig. 4. TEM photomicrograph of as-deposited 50-Å Nb_2O_5 films, inertly sputtered (a) 50(—,A), and reactively sputtered (b) 50(—,O). The IS film has contrast features due to "island" formation during sputter deposition not seen in the RS film, indicating different growth mechanisms of the as-deposited films. The IS films grow by an island mechanism (Volmer–Weber type growth) while the RS films grow more nearly layer-by-layer (Frank–van der Merwe type growth). See text for details.

for all the as-deposited films, but was observed most clearly in the thickest films, as in Fig. 4.

After deposition and removal from the sputtering chamber, all sputtered niobium films, both IS and RS, were found to contain fully oxidized niobium (Nb^{5+}) as determined by XPS, with no evidence for niobium in any other oxidation state. The binding energy for Nb^{5+}, the Nb($3d_{5/2}$) signal, referenced to the C(1*s*) peak at −284.6 eV, was between −207.0 and −207.5 eV for all the samples examined, which agrees well with the accepted range of −207.0 to −207.4 eV (*23*). XPS did not detect other elements in these samples with the excep-

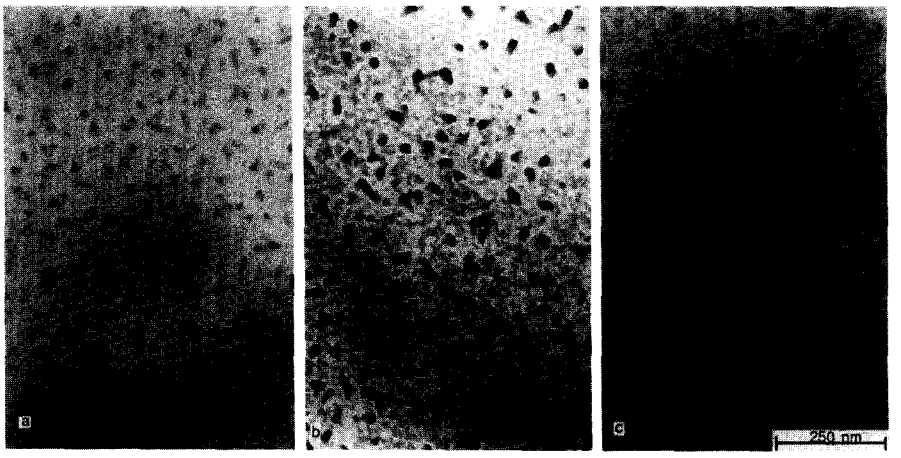

Fig. 5. TEM photomicrograph of inertly sputtered films treated at 873 K for 2 h. All three have crystals of only H-Nb_2O_5, the amount and size of which increases with initial Nb_2O_5 thickness from 4 Å, (a) 4(600,2,A), through 12 Å, (b) 12(600,2,A), to 50 Å, (c) 50(600,2,A). The differences in overall contrast level of the micrographs and relative contrast of the H-Nb_2O_5 crystallites are due to the different silica film thicknesses and slightly different imaging conditions used.

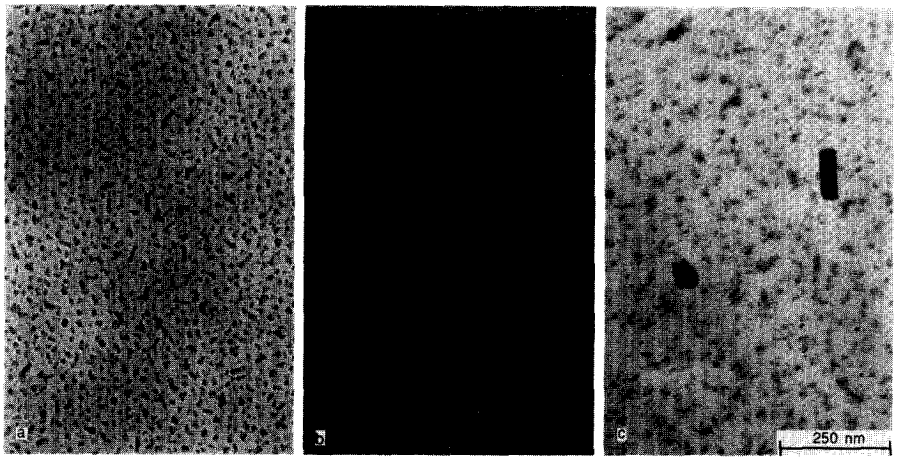

Fig. 6. TEM photomicrograph of reactively sputtered monolayer Nb_2O_5 films heated at 873 K, showing the development of niobia crystallization. T-Nb_2O_5 occurs in (a) 4(600,2,O) and (b) 4(600,6,O); both T- (lighter) and H-Nb_2O_5 (darker contrast) are in (c), 4(600,16,O). The differences in overall contrast levels of the three micrographs are due to varying silica film thicknesses.

tion of minor C contamination, which was easily removed by sputtering. Grunder and Halbritter have found that niobium spontaneously oxidizes to depths of approximately 6 nm in air at room temperature (*24, 25*), supporting the observation of the as-deposited films being fully oxidized after exposure to oxygen.

After heat treatment at 773 and 873 K for 2, 6, and 16 h, both the IS and RS films were examined by TEM. Representative micrographs are shown in Figs. 2 and 5 for the IS films, in Figs. 3 and 6–8 for the RS films. Figure 2 is typical of all three thicknesses (4, 12, and 50 Å) of IS films treated at 773 K, while Fig. 3 is representative of RS films treated at 773 K. As seen in Figs. 2 and 3, there is an appearance of contrast features with continued heat treatment time. This behavior is also noted in the 12-

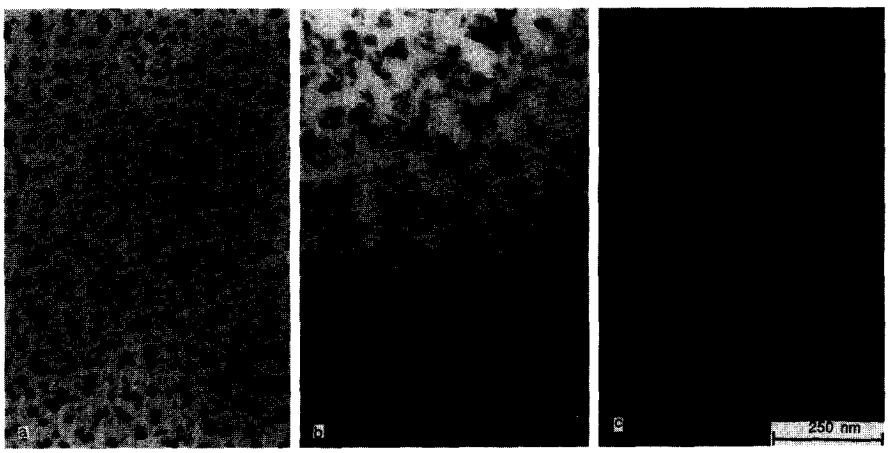

Fig. 7. TEM photomicrograph of reactively sputtered 12-Å Nb_2O_5 films heated at 873 K. The 12-Å films develop larger and more extensive H-Nb_2O_5 crystals than the monolayer (4-Å) films, compared with Fig. 6, as there is more "free" niobia in the 12-Å films. (a) has T-Nb_2O_5, while both (b) and (c) contain T- (lighter) and H-Nb_2O_5 (darker contrast). (a) 12(600,2,O), (b) 12(600,6,O), (c) 12(600,16,O).

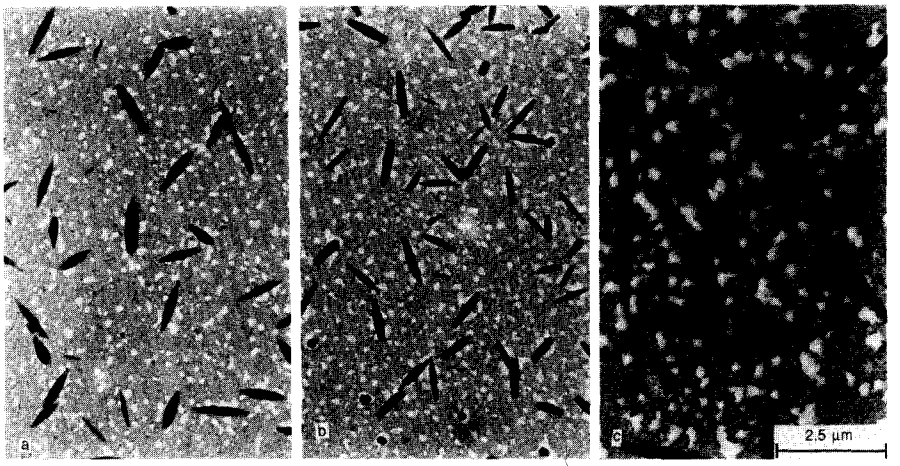

Fig. 8. TEM photomicrograph of reactively sputtered 50-Å Nb_2O_5 films heated at 873 K. All three contain microcrystalline, indistinct T-Nb_2O_5 (continuous appearing medium contrast) and well-crystallized H-Nb_2O_5. Heating times range from 2 h (a) 50(600,2,O), through 6 h (b) 50(600,6,O), to 16 h (c) 50(600,16,O). These films should be compared with those depicted in Figs. 6 and 7 for the effects of increasing film thicknesses on niobia crystal development. In these micrographs, both T- and H-Nb_2O_5 are more extensive because of the availability of more niobia for crystallization. The relative amount of H-Nb_2O_5 is seen to increase with longer heating times.

and 50-Å films, and is interpreted as agglomeration of niobia into "islands" on the surface of the silica. No crystallinity could be observed in electron diffraction patterns obtained from regions containing the islands, in all of the RS films and also for the IS films heated for at least 6 h. After 16 h these islands became much darker on the IS films (Figure 2c) and gave rise to weak crystalline diffraction patterns.

Figures 6, 7, and 8 illustrate the changing appearance of the RS films with respect to both heating times at 873 K and film thickness. As time and thickness were increased, crystallites on the samples became more clearly developed and larger. The same behavior was found for the IS films, as seen in Fig. 5.

At least two different crystalline phases of niobia were detected by TED, depending on film thickness, heating time and temperature, and sputtering environment. Diffraction patterns corresponding to these two phases are shown in Fig. 9, together with a pattern showing amorphous scattering from silica (Fig. 9a). One phase was seen to

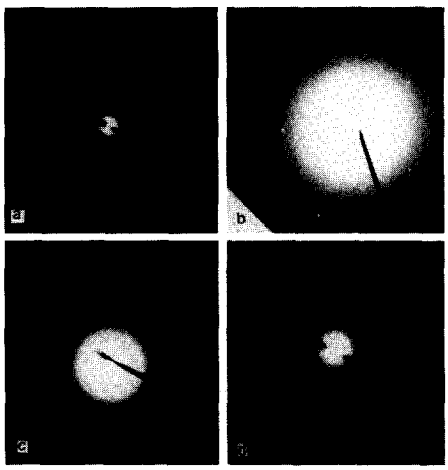

Fig. 9. Representative transmission electron diffraction patterns from selected samples. (a) is amorphous silica, (b) is a spot pattern corresponding to H-Nb_2O_5, and is taken from 12(600,6,A), (c) is a weak ring pattern corresponding to T-Nb_2O_5, taken from 12(600,2,O), and (d) correpsonds to T-Nb_2O_5 from an HSA sample, NSIII (600,16). In all patterns, the intense central spot arises from amorphous diffraction from the silica support and significantly distracts from available information.

produce either distinct spot patterns, as illustrated for 12(600,6,A) in Fig. 9b, or combinations of spotty ring and multiple spot patterns. The other phase occurred exclusively as weak ring patterns, where typically only the two to three strongest reflections were found, as seen in Fig. 9c for 12(600,2,O).

Niobia occurs in a multiplicity of phases, most of which are metastable. An excellent review which simplifies and clarifies the complex nomenclature of Nb_2O_5 phases was published by Schafer *et al.* (*26*) and recently summarized by Burke (*27*). The phase producing ring patterns exclusively, as in Fig. 9c, has *d*-spacings corresponding to those of either T- (*29*) or TT-Nb_2O_5 (*28*). These phases were named by the German workers, and signify the low- (*tief*) and very-low- (*tief-tief*) temperature forms of Nb_2O_5. TT-Nb_2O_5 first crystallizes at about 673 K from amorphous Nb_2O_5, while T-Nb_2O_5 forms from TT-Nb_2O_5 at slightly higher temperatures (*26*). Subsequent observations on pure T- and TT-Nb_2O_5 produced in our laboratory have shown that these phases are most likely identical and represent different degrees of crystal perfection moderated by the presence of impurities, rate of crystallization, and other factors (*30*). This phase, characterized by weak ring TED patterns, is called T-Nb_2O_5 in this paper.

The situation is more complicated for the phase having the diffraction pattern illustrated in Fig. 9b. While about a dozen *d*-spacings could be measured from this pattern, four Nb_2O_5 phases, H-, B-, N-, and M-Nb_2O_5, have d-spacings sufficiently close that any of them might fit the observed diffraction pattern (*31–37*). Experimental and literature *d*-spacings are compared in Table 1. While either H- or M-Nb_2O_5 gives the best fit to the experimental data, the observed phase will be considered as the most stable under the experimental conditions used, H-Nb_2O_5 (*30*).

The phases found by TED in the TF samples are summarized in Table 2. Some samples were found not to have distinct crystalline features in the TED patterns and are indicated by dashes. Other samples contain one or both of T- and H-Nb_2O_5. A few samples had crystalline diffraction patterns too weak for positive identification; these are indicated by "X." At 873 K the IS samples were found to be exclusively H-Nb_2O_5, while the RS samples contained both T- and H-Nb_2O_5.

The different types of diffraction features arising from the two phases are due to the

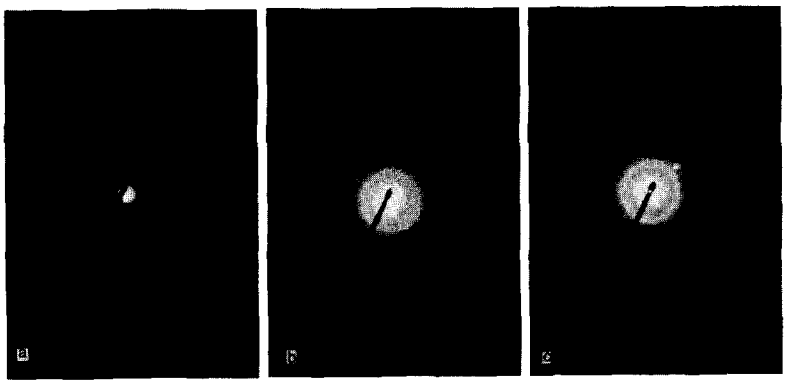

Fig. 10. Electron diffraction patterns corresponding to the samples shown in Fig. 8. The rings are diffractions from T-Nb_2O_5, while the spots arise from H-Nb_2O_5 and the broad ring and central spot are amorphous diffractions from the silica support. With increasing heating time, from (a) to (c), the relative intensity of H-Nb_2O_5 increases, while T-Nb_2O_5 intensity remains about the same, indicating the growth of H-Nb_2O_5 crystals with time.

TABLE 1

Experimental and Literature Values of *d*-Spacings and Relative Intensities for Niobia[a,b]

12(600,6,A)[c,d]		50(600,16,O)[c,d]		H-Nb_2O_5(31)[e,f]		M-Nb_2O_5(34)[e]		N-Nb_2O_5(33)[e,g]		B-Nb_2O_5(37)[e]	
d(Å)	*I*	*d*(Å)	*I*	*d*(Å)	*I*	*d*(Å)	*I*	*d*(Å)	*I*	*d*(Å)	*I*
		3.88	m	3.83	<10	3.86	10[h]	—		—	
		3.75	m	3.75	70	3.75	s	3.77	s	—	
				3.74	50						
3.66	m			3.65	100	3.64	50[h]	—		3.64	80
3.61	w			3.56	<10	3.59	s	3.59	m	—	
3.30	m			3.28	<10	3.36	w	—		3.32	65
		3.21	vs	3.17	<10	3.16	10[h]	3.22	vvw	3.08	100
		3.16	s					3.18	w		
		2.94	w	3.01	<10	—		2.92	vw	2.98	80
		2.90	w	—		—		2.88	vw	—	
2.85	s			2.84	10	2.79	m	2.84	vw	—	
				2.83	10						
		2.70	w	2.71	20	2.70	30[h]	2.68	vw	2.69	45
		2.60	s	2.55	10	2.54	w	2.59	w	—	
2.26	w			2.32	10	2.32	m			2.22	14
1.94	m	1.94	m	1.92	20	1.91	s			1.96	30
1.78	m	1.87	vw	1.82	10	1.78	w			1.81	45
				1.79	10					1.81	35
				1.74	10					1.72	10
1.73	m	1.76	m	1.69	10	1.70	vw			1.71	20
1.69	m	1.75	w	1.69	10					1.70	55
1.60	w	1.61	m	1.58	10	1.58	m			1.61	7
1.57	w	1.60	m	1.56	10					1.57	6

[a] Intensities are given either numerically, with most intense peak = 100; otherwise letters indicate vs, very strong; s, strong; m, medium; w, weak; vw, very weak.

[b] Only those *d*-spacings which might correspond to experimental *d*-spacings are reported here. Dashes indicate no reported spacing which matches experimental value.

[c] Obtained by electron diffraction.

[d] *d*-spacings for the two experimental measurements differ as crystals in different orientations were used to obtain the given TED pattern. The error for these measured values is about 5%.

[e] Obtained by X-ray diffraction.

[f] Called α-Nb_2O_5 by Holtzberg *et al.* (*31*).

[g] No *d*-spacings reported below 2.51 Å.

[h] Additional *d*-spacings taken from Ref. (*35*).

size of the crystallites present. T-Nb_2O_5 occurs exclusively as randomly oriented microcrystalline aggregates, which produce rings in the diffraction patterns. The size of the H-Nb_2O_5 crystals varies from 100 to over 10,000 Å, as seen in the series of micrographs (Figs. 6–8), with the largest crystals occurring on those samples having the thickest films and longer heating times, as shown in Fig. 8. Corresponding diffraction patterns showing this same trend are shown in Figure 10.

Crystalline niobia on the IS films also gave rise to ring and spot features in the same diffraction pattern; however, both can be assigned to H-Nb_2O_5. In Fig. 5b, for example, regions of both more- and less-well-crystallized H-Nb_2O_5 are visible. In both IS and RS films there are regions where the silica appears to be completely dewetted, most clearly illustrated in the 50-Å RS films (Fig. 8). Whether these regions are completely devoid of niobia is not known, as TEM is not sensitive enough to reveal monolayers. However, mass balance considerations on the monolayer (4-Å) film

TABLE 2

Phases Found by TED in TF Samples

Treatment	Phase(s) observed[a]					
	Inertly sputtered			Reactively sputtered		
	4 Å	12 Å	50 Å	4 Å	12 Å	50 Å
(500,2)	—	—	—	—	—	—
(500,6)	—	—	—	—	—	—
(500,16)	—	—	X	—	—	—
(600,2)	X	H	H	T	T	T + H
(600,6)	H	H	H	T	T + H	T + H
(600,16)	H	H	H	T + H	T + H	T + H

[a] Dashes, no crystalline features observed; X, crystalline; T, T-Nb_2O_5; H, H-Nb_2O_5.

lead to the conclusion that if bulk niobia crystals are formed, then niobia must at least partially dewet regions of the silica film in order to support crystal growth.

High-surface-area samples. The HSA samples were examined by TEM and the results are presented in Figs. 9d, 11, and 12 and in Table 3. Bare silica is compared with NSI (500,2) and NSIII (500,2)[2] after the initial calcining step in Fig. 11. No additional contrast features can be observed because of the presence of niobia, and these samples were amorphous by electron diffraction.

[2] In the HSA samples, NSI refers to a monolayer of Nb_2O_5 on silica, while NSIII indicates three layers. (500,2) indicates heating at 773 K for 2 h.

TABLE 3

Phases Found by TED in HSA Samples

Treatment	Phase observed[a]	
	One monolayer	Three monolayers
(500,2)	A	A
(600,2)	A	T
(600,16)	T	T

[a] A, amorphous; T, T-Nb_2O_5.

The NSI (600,2) and NSIII (600,2) samples appeared very similar to the corresponding (500,2) samples. While no crystalline contrast was observed directly, the TED pattern showed that NSI (600,2) was amorphous, while NSIII (600,2) had a faint diffraction pattern corresponding to T-Nb_2O_5. The (600,16) samples are presented in Fig. 12. Figures 12a and 12c are NSI and NSIII at the same magnification as in the other micrographs; Figs. 12b and 12d were taken at the highest practical resolution of the microscope.

Both NSI (600,16) and NSIII (600,16)

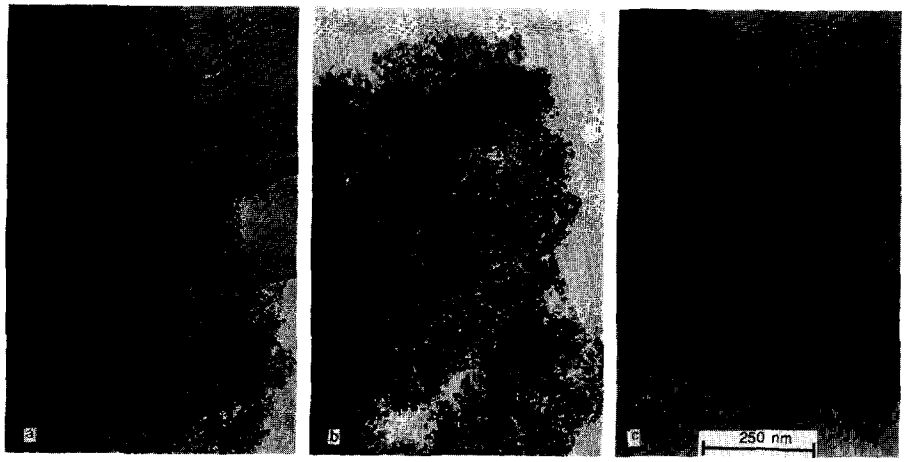

Fig. 11. TEM photomicrograph of high-surface-area samples. (a) is HSA silica as received, while (b), NSI (500,2), and (c), NSIII (500,2), contain one and three monolayers of Nb_2O_5, respectively, after the initial calcining step. Little difference is seen in the appearance of the three samples in spite of the presence of niobia.

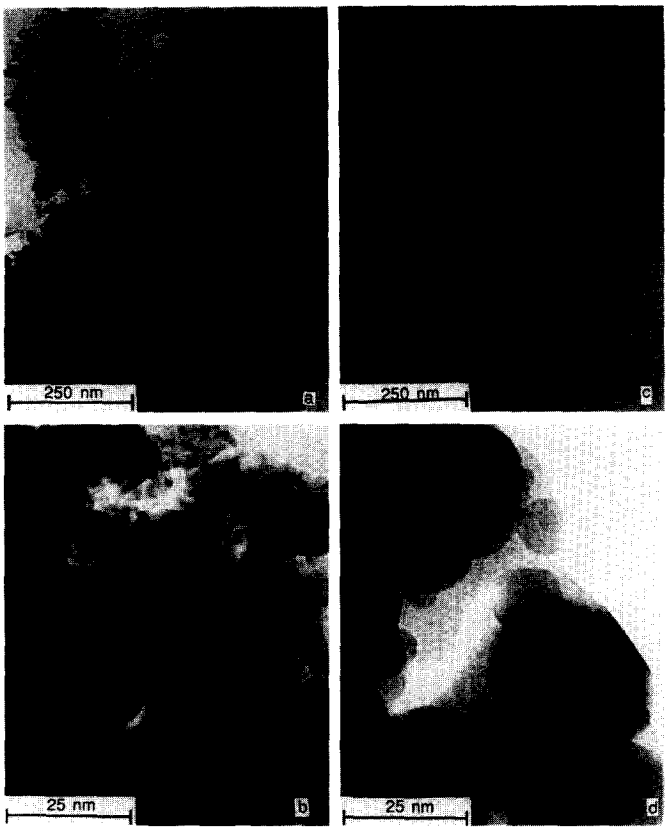

Fig. 12. TEM photomicrographs of high-surface-area samples, showing extent of crystallization at 873 K after 16 h for the one- and three-monolayer samples. (a) and (c) are NSI (600,16) and NSIII (600,16), respectively, and (b) and (d) correspond to the same samples at higher (10×) magnification. Both samples contain T-Nb_2O_5, seen as the vague darker spots in (b) for the monolayer sample, and as well developed crystals in (d) for the three-layer sample.

proved to contain T-Nb_2O_5 crystals. The darker spots in Fig. 12b correspond to crystallites in NSI. NSIII (Fig. 12d) is seen to consist of relatively larger well-developed crystals with connecting amorphous regions. The crystals appear to be tabular and very thin, as details of individual overlapping crystals can be easily observed. The diffraction pattern from NSIII (600,16) is given in Fig. 9d, and is typical of all HSA samples containing T-Nb_2O_5. This pattern is similar to that of the T-Nb_2O_5 TF samples, but in this case the rings have a greater intensity as more diffracting crystals are present. Again, the presence of rings rather than spots is indicative of the presence of small crystals.

These results are similar to what was found earlier by XRD (*16*). The differences from the earlier study are easily explained by the resolution of the two techniques used. While the resolution of TED is poorer, as only three spacings were observed, the technique allows for the identification of much smaller particles. NSI (600,16) has particles too small for detection by XRD and these are barely discernible in the TEM micrographs in Fig. 12b, although TED was possible from these particles.

DISCUSSION

The observation that the HSA and TF samples behave similarly, but not identi-

cally, toward heat treatment is significant. These subtle differences are indicative of different degrees of interaction between the niobia and silica, depending on the silica substrate used and the exact mode of niobia deposition. While the formation of niobia aggregates, either amorphous or crystalline, was observed in all the monolayer TF samples, no such formation was observed in the NSI samples. In addition, no niobia aggregates could be observed on the NSIII samples treated at 773 K, while niobia crystals were observed in the same samples at 873 K.

The results from the TF samples indicate that niobia dewets silica, even at monolayer coverage. What cannot be observed from TEM observations alone is the extent of this dewetting and whether dewetting occurs on the HSA samples, especially the NSI sample. If monolayer niobia on HSA silica is unstable with respect to heat treatment, these materials may not be useful as catalysts and catalyst supports, as the exposed silica is likely to influence the resultant catalytic chemistry. While previous observations have indicated the monolayer to be stable, no direct evidence was presented (*16*). The following sections attempt to address this issue.

Another feature not immediately apparent from the TEM micrographs is the stability of the monolayer in the presence of niobia above this amount. While multilayer niobia forms amorphous or crystalline aggregates, as in the TF samples and NSIII (600,2), whether monolayer niobia will also dewet the surface and join the aggregation is not clear. This issue represents a tradeoff between the minimization of surface free energy and other interactions, such as chemical bonding between surface-phase niobia and silica. By comparison of the behavior of the two types of samples examined, the problem of stability of a monolayer in the presence of bulk niobia can also be discussed.

Monolayer behavior: high-surface-area samples. As shown above, NSI was amorphous after treatment at both 773 and 873 K, with the exception of the (600,16) sample, which was found to be weakly crystalline as T-Nb_2O_5. Silica apparently stabilizes NSI from the crystallization observed in NSIII. Mechanisms for surface interaction proposed for similar systems can be used to explain such a stabilization, as discussed below.

Vanadium salts have been shown to bond to the surfaces of numerous oxide supports, such as Al_2O_3, TiO_2, and SiO_2, after impregnation and calcination, by a surface hydroxyl extraction mechanism (*4, 7, 14, 38, 39*). Thus a direct surface metal-to-oxygen-to-vanadium (M–O–V) bond is formed, which serves to "anchor" the precursor vanadium salt as well as subsequent vanadium oxide to a specific surface site of the support. A one-to-one stoichiometry of V atoms to surface OH groups was noted by these workers. Samples containing V_2O_5 below and up to the monolayer coverage were amorphous by XRD after mild calcination (673 K, 2 h), while samples containing an excess of V_2O_5, above the monolayer amount, were found to contain crystalline V_2O_5 by XRD and other methods (*11, 14*). Similar results have been found for MoO_3 on SiO_2 (*12*), MoO_3 on ZrO_2 (*40*), WO_3 on Al_2O_3 (*13, 41*), MoO_3 on Al_2O_3 (*10*), and MoO_3 on TiO_2 (*11*).

For our Nb_2O_5–SiO_2 system, we propose that the reaction of niobium ethoxide and silica proceeds via a surface hydroxyl reaction mechanism as well. This results in a Nb–O–Si linkage in the anchored precursor, which is converted to surface niobia in the subsequent calcining step. Although the exact chemistry and the nature of the anchored species are unknown, this postulates identifies the importance of oxygen linkages and, in essence, surface hydroxyl groups in the preparation of surface oxides. In their recent work on model thin films consisting of molybdenum oxide supported on alumina, Hayden and Dumesic (*42*) also noted the effect of Mo–O–Al linkages on the morphology of the supported phase.

As mentioned earlier, crystallites of T-Nb_2O_5 are found for the NSI (600,16) sample, while other NSI samples remain amorphous. One explanation is that the surface-phase niobia can be made to partially dewet with a sufficiently severe heat treatment. Another explanation has to do with the measured BET surface areas of NSI (500,2) and NSI (600,16), which are 377 and 304 m^2/g SiO_2, respectively (*16, 27*). It is likely that with the loss in surface area of the sample, some niobia above the monolayer amount is transformed into T-Nb_2O_5. Even though present data cannot eliminate either of these possibilities, the observed behavior of the NSI (600,16) sample is consistent with the main conclusion of the above model. Specifically, the surface phases in the HSA samples are more stable than their TF counterparts under similar treatments. The role of surface hydroxyls in affecting the sintering and crystallization behavior of niobia supported on thin films is discussed below.

Monolayer behavior: Thin film samples. The differences between the reactively sputtered (RS) and inertly sputtered (IS) monolayer thin film samples further clarify the behavior of the HSA samples. As seen most clearly in Fig. 4, the IS as-deposited film (Fig. 4a) shows a texture not seen in the RS as-deposited film (Fig. 4b), and is indicative of film dewetting. The IS film probably grows by an island type mechanism (similar to Volmer–Weber growth), while the RS films are formed in a more nearly layer-by-layer (Frank–van der Merwe growth) manner, as described by Bauer and Poppa (*43*). A good assumption for the IS case is that, like most high-melting-point metals, as-deposited niobium will only partially wet the silica surface. Thus, niobium is expected to form islands on silica.

The situation is different in the RS film, as seen by the absence of islands in the as-deposited morphology. Nb_2O_5 films as deposited have been found to be oxygen deficient (*44, 45*). Based on this observation an assumption can be made that the presence of oxygen in the sputtering gas leads to the formation of NbO_x free radicals. When the NbO_x radicals encounter the surface they stand a better probability of reacting with the surface. The reaction probably also involves surface hydroxyl groups, as in the case of HSA samples. As a consequence, the RS films can be more firmly attached to the silica surface, leading to Nb–O–Si linkages, than their counterpart IS films.

The response to heat treatment of the two series of samples is dependent on this initial difference in film structure. While both IS and RS films show dewetting when treated at 773 K (Figs. 2 and 3), the dewetting is more dramatic for the IS case, and leads to the formation of poorly crystallized particles after 16 h of treatment. The crystallized aggregates could not be observed in the RS case, consistent with the assertion that niobia is more strongly held to the surface on the RS films.

Effects of surface interaction on phase stability. At 873 K, the difference between the two series of monolayer TF samples is even more dramatic. On the IS samples, H-Nb_2O_5 was formed, while on the RS samples, both T- and H-Nb_2O_5 was found (Table 2). Recalling that T-Nb_2O_5 was the only phase found on the HSA samples, we can summarize the behavior of the three series of samples with the important observation that *the stronger the interaction between the support and the surface oxide, the more dramatic is the effect on the surface oxide*. This interaction leads to the inhibition of crystallization to the more stable H-Nb_2O_5 in NSIII and the prevention of crystallization in the case of NSI, with the concomitant formation of surface-phase niobia. The interaction is seen to be weak in the IS TF samples, moderate in the RS TF samples, and strong in the HSA samples. Previous workers have also pointed to the effects of support/surface oxide interactions and their influence on surface behav-

ior, especially for the case of V_2O_5 on different titanias (*1, 2, 8, 9*).

The physical basis for the varying strength of interaction in these series of samples needs to be identified. Perhaps the most important difference between the HSA and TF silica support is that the TF silica support was treated at 1000°C prior to niobia deposition. A well-known feature of silica with respect to heat treatment is permanent dehydroxylation of the surface with increasing temperature. Iler reports at least an 80% loss in surface OH content when silica is heated to 700°C or higher temperatures (*46*). The TF silica is likely to have fewer surface hydroxyls, on a per surface area basis, than the as-received HSA silica, which is fully hydroxylated.

These observations are consistent with the earlier postulate that the number of surface hydroxyls is an important parameter in controlling the extent of interaction on the different supports. The HSA supports, with a high concentration of surface hydroxyls, enable a firm anchoring of the precursor and the subsequent stabilization of surface-phase niobia through Nb–O–Si linkages. The TF supports show either weak or no interaction with niobia as they have correspondingly less surface OH. Niobia on the IS films does not interact with the silica surface, as the initial deposition was in the form of metallic dewetted islands. Apparently when the metallic niobium is oxidized, the oxidation product, Nb_2O_5, remains inert with respect to the support. The RS films develop a moderate interaction with the surface, as in this case niobia is envisioned to be deposited as reactive molecules, but the interaction is limited by the lack of surface hydroxyls on the TF silica surface.

This model satisfactorily explains the behavior of niobia surface oxides, summarized in Table 4. "Free" niobia, as on IS-TF, crystallizes to H-Nb_2O_5. Niobia in the presence of surface-phase niobia, which is chemically held to the surface, forms T-Nb_2O_5, as in HSA. RS-TF is intermediate between these two extremes. Apparently three types of niobia can occur on silica, with differing degrees of interaction with the surface.

Similar observations have been reported for other systems. For chromia on silica, Richter *et al.* (*47*) have compared their work with previous studies. They found that at low CrO_3 coverages, CrO_3 is stabilized toward reduction. At higher coverages, they found the presence of both small clusters (oxyspecies) and "bulk-like" amorphous surface phases. When heated

TABLE 4

Summary of Differences in the Three Series Examined

	HSA	RS-TF	IS-TF
Si-OH groups/nm^2 on surface	High	Low	Low
As-deposited chemistry	$(OC_2H_5)_x$Nb-O-Si[a]	O_xNb-O-Si[a] + O_xNb/HO-Si[b]	Nb/HO-Si[b]
4- and 12-Å film behavior at 773 K	Apparently stable	Dewets	Dewets
Monolayer behavior after 873 K, 2 h	(No crystallinity observed)	Forms T-Nb_2O_5	Forms H-Nb_2O_5
12-Å film behavior after 873 K, 2 h	Forms T-Nb_2O_5	Forms T-Nb_2O_5	Forms H-Nb_2O_5

[a] x denotes uncertainty in stoichiometry.
[b] A / indicates no interaction.

above 575 K, the oxyspecies remained stable while the bulk CrO_3 was reduced to crystalline Cr_2O_3. This shows that CrO_3 forms both "interacting" and "noninteracting" states on SiO_2. Similarly, for CoO on ZrO_2, Bettman and Yao proposed a dynamic equilibrium between surface and bulk phase CoO on ZrO_2, which could be adjusted by varying the CoO coverage (*48*). Hayden and Dumesic (*42*), in a study using thin film samples, found that Mo oxide species are highly dispersed on alumina for loadings below ca. 5 Mo atoms/nm^2. Above this loading both highly dispersed species and orthorhombic MoO_3 crystallites exist.

Different degrees of interaction are important not only in considering the relationship between structure and coverage, as in the examples cited above, but also in comparing samples prepared by different methods. V_2O_5 on TiO_2 was found to be unstable in the TEM by Vejux and Courtine (*1*) but not by Kang and Bao (*2*). In the first case, V_2O_5 was vapor deposited whereas in the second case, V_2O_5 was prepared through aqueous impregnation of vanadium oxalate followed by calcination. In light of the above results, one would expect a stronger interaction from the second preparation method, which gives a more stable sample when exposed to heating effects in the electron microscope.

Multilayer film behavior. The above model can be extended to account for the behavior of the multilayer HSA and TF samples. The main difference between the monolayer and multilayer films is that while monolayer niobia is stabilized by the surface as a surface phase, as in the NSI samples, multilayer niobia is able to adopt a more stable bulk form.

In the HSA samples, subsequent Nb_2O_5 layers are most likely deposited in the same manner as the monolayer, which involves the abstraction of surface hydroxyls and formation of metal–oxygen–metal linkages. The difference is that for the monolayer, Nb–O–Si bonds are formed, while for the second and third layers, Nb–O–Nb bonds occur, as in the mechanism proposed for multilayer V_2O_5/TiO_2 systems (*38*). One reason for weakening of the multilayers is that impregnation of additional layers may not be stoichiometric (*7*), the consequence of which is that unreacted OH groups attached to niobium atoms may remain and be contained in the multilayer films. Fehlner and Mott have noted that the introduction of water and M–OH groups reduces the average bond strength in glass formers (such as SiO_2 and Nb_2O_5) and increases the rate of reordering in the oxide structure (*49*). This destabilization of the multilayer films could be responsible for the crystallization observed in the NSIII samples.

Surface-phase niobia has been demonstrated to be highly stable. In all probability, the surface phase remains stable even in the multilayer HSA samples. If the surface phase had become destabilized by the presence of additional niobia above monolayer coverage, then behavior similar to that of the TF samples would have been observed. The presence of H-Nb_2O_5 is indicative of destabilized dewetted niobia. H-Nb_2O_5 was not found on the HSA samples, indicating that the surface phase remains stable under all experimental conditions and niobia film thicknesses.

In the TF samples, the behavior observed for the multilayers is the same as in the monolayer samples; the presence of additional amounts of niobia serves only to make the phenomenon easier to observe. With increasing time and temperature, larger and more numerous crystallites or amorphous aggregates are found in the 12- and 50-Å samples, as compared to the 4-Å TF, with the exact phase observed depending on the conditions used. These differences between the TF and HSA samples are outlined in Table 4. On the 50-Å RS samples, enough excess niobia is present from the start so that H-Nb_2O_5 forms earlier than in the other RS samples. T-Nb_2O_5 in the RS–TF samples indicates that some niobia is present as a surface phase on these samples and remains stable under all condi-

tions examined, as does the HSA surface-phase niobia. The presence of T-Nb_2O_5 is indicative of crystallization of niobia over surface-phase niobia.

Phase stabilization in niobia films. Both T- and H-Nb_2O_5 are found in the RS TF samples, but only H-Nb_2O_5 is found on the IS TF and only T-Nb_2O_5 is found on HSA supports. The different phases stabilized are due to the extent of interaction with the amorphous silica support. The preferred state of niobia on silica, at 873 K, is dewetted crystals of H-Nb_2O_5. Although both are oxides, niobia does not wet silica nor does niobia interact with silica, as shown by the following observations. The phase diagram for the Nb_2O_5/SiO_2 system shows complete immiscibility over all compositions in the solid state, and significant immiscibility in the liquid state (*50*). In Fig. 8, the large H-Nb_2O_5 crystals are clearly seen as lying over the surface, with poorly crystalline regions of T-Nb_2O_5 and open areas of silica visible *through* the H-Nb_2O_5 crystals, again indicating no interaction between stable H-Nb_2O_5 and the surface. Pressure/temperature diagrams for Nb_2O_5 show that at lower pressures and at temperatures above 750°C the equilibrium phase is H-Nb_2O_5; below 750°C the most stable phase is B-Nb_2O_5 (*37*). However, phase transitions between some of the different polymorphs of niobia are sluggish. The stability of T-Nb_2O_5 may be enhanced by several factors, including interactions with the silica surface and a slow rate of transformation to a more stable phase.

H-Nb_2O_5 is the more stable phase at the crystallization conditions, but T-Nb_2O_5 is also found, perhaps indicating that there is an interaction with the surface that stabilizes T-Nb_2O_5. T-Nb_2O_5 has coordinated six- and seven-fold niobium with oxygen, arranged in an irregular manner so that the occupancy factor for any given niobium atom site is never greater than 0.5 (*51, 52*). The structure of H-Nb_2O_5, in contrast to that of T-Nb_2O_5, consists of highly ordered blocks of NbO_6 octahedra with regularly placed tetrahedral Nb (*53, 54*). The irregular structure of T-Nb_2O_5 may be more flexible and allow for at least a partial incorporation of Nb–O–Si bonded surface-phase niobia into the structure, which has only a limited mobility, being randomly attached to an amorphous silica support. Niobia oxygen-linked to the amorphous silica surface is likely to force additional niobia, situated near or on top of the surface-phase niobia, to crystallize into T-Nb_2O_5. In other words, surface niobia acts as a template for T-Nb_2O_5 formation. This will account for the absence of the H phase in the HSA samples, on which the surface is fully hydroxylated and is able to bond to a full surface-phase niobia layer. Excess niobia, as in the NSIII samples, while having sufficient mobility to form crystallites, is prevented from crystallizing to H-Nb_2O_5 by the underlying disordered surface-phase niobia.

The TF series presents a somewhat different situation. In the RS samples, only part of the surface is covered with stable, Nb–O–Si bonded niobia because of the much lower silica surface OH concentration. Niobia in the neighborhood of surface-phase niobia dewets the surface and is forced into crystallizing as T-Nb_2O_5, as in the 4(600,2,O) sample. Additional niobia present away from the surface phase dewets and forms the preferred H-Nb_2O_5 phase. In the IS samples, no niobia is held to the surface, so all forms H-Nb_2O_5.

On the basis of the above arguments for phase stabilization, T-Nb_2O_5 should be expected to form smaller crystals, as T-Nb_2O_5 is intimately associated with surface structure on the molecular scale. H-Nb_2O_5 forms much larger crystals, as this form is found when niobia is not associated with the surface or surface-phase niobia. The electron diffraction patterns from the TF and HSA samples bear out this observation, as seen in Figs. 9 and 10.

Crystallization was not observed in any of the samples heated to 773 K, with the exception of the IS–TF samples heated for

16 h. The TF samples would be expected to crystallize, as islands of dewetted niobia were observed in these samples. These islands may represent areas that have crystallized, but the sizes of which were too small to produce detectable coherent scattering in the TEM. Another equally likely possibility is that the kinetics of crystallization is too slow at 773 K to produce observable crystals within the time limitations of the experiment. Thus even in the 16-h IS–TF samples, which contained the most moblie Nb_2O_5, only poorly developed crystallization was observed.

SUMMARY

This study illustrates the usefulness of model thin films in understanding the behavior of oxide catalytic materials. Our results have shown that the influence of the support and preparation on the structure of surface oxides can be dramatic. Monolayer surface-phase niobia can be stabilized on high-surface-area silica, as the amorphous silica support contains surface hydroxyl groups which develop Nb–O–Si linkages for stabilization. The surface-phase niobia is stable to further heat treatments and can influence the morphology and structure of subsequently deposited niobia, above the monolayer amount, as revealed by the formation of microcrystalline T-Nb_2O_5.

The presence of two crystalline niobia species, T and H, on the model thin films indicates that only part of the niobia is surface-stabilized on these supports, as T-Nb_2O_5 is found to be stabilized by incorporating surface-phase niobia. On samples prepared in such a way as to prevent surface interactions from occurring, through deposition in an inert atmosphere, only H-Nb_2O_5 was formed, and the presence of this phase indicates a very weak interaction between niobia and the surface.

The hypothesis presented here, which points to surface hydroxyl groups as important in stabilizing surface-phase oxides in both wet and dry preparation methods, is appealing in its simplicity. We have proposed a single model which gives a consistent picture of the stability and crystallization of single and multiple layers of niobia on silica in low- and high-surface-area samples. The identification of this important parameter will allow not only a better control of the preparation of similar oxide–oxide systems, but also a more meaningful comparison of results from different laboratories in terms of the extent of interaction between the surface oxide and the support.

ACKNOWLEDGMENTS

This work was supported by the Center for the Study of Materials at Carnegie Mellon University under Grant DMR-8521805. The help of Roland Schulz at the University of Minnesota Surface Analysis Center in obtaining XPS data is appreciated; many helpful discussions with Peter Burke are also appreciated.

REFERENCES

1. Vejux, A., and Courtine, P., *J. Solid State Chem.* **63,** 179 (1986).
2. Kang, Z. C., and Bao, Q. X., *Appl. Catal.* **26,** 251 (1986).
3. Inomata, M., Mori, K., Miyamoto, A., Ui, T., and Murakami, Y., *J. Phys. Chem.* **87,** 754 (1983).
4. Glinski, M., and Kijenski, J., *in* "Preparation of Catalysis III" (P. Grange and P. A. Jacobs, Eds.), p. 553. Elsevier, Amsterdam/New York, 1983.
5. Inomata, M., Mori, K., Miyamoto, A., and Murakami, Y., *J. Phys. Chem.* **87,** 761 (1983).
6. Haber, J., Kozlowski, A., and Kozlowski, R., *J. Catal.* **102,** 52 (1986).
7. Kijenski, J., Baiker, A., Glinski, M., Dollenmeier, P., and Wokaun, A., *J. Catal.* **101,** 1 (1986).
8. Murakami, Y., Inomata, M., Mori, K., Ui, T., Suzuki, K., Miyamoto, A., and Hattori, T., *in* "Preparation of Catalysts III" (P. Grange and P. A. Jacobs, Eds.), p. 531. Elsevier, Amsterdam/New York, 1983.
9. Saleh, R. Y., Wachs, I. E., Chan, S. S., and Chersich, C. C., *Prepr. Amer. Chem. Soc. Div. Pet. Chem.*, 272 (1986).
10. Zaki, M. I., Vielhaber, B., and Knozinger, H., *J. Phys. Chem.* **90,** 3176 (1986).
11. del Arco, M., Holgado, M., Martin, C., and Rives, V., *J. Catal.* **99,** 19 (1986).
12. Brito, J., and Laine, J., *Polyhedron* **5,** 179 (1986).
13. Salvati, L., Makousky, L. E., Stencel, J. M., Brown, F. R., and Hercules, D. M., *J. Phys. Chem.* **85,** 3700 (1981).
14. Busca, G., Certi, G., Marchetti, L., and Trifiro, F., *Langmuir* **2,** 568 (1986).

15. Moggi, P., and Albanesi, G., *React. Kinet. Catal. Lett.* **22,** 247 (1983).
16. Ko, E. I., Bafrali, R., Nuhfer, N. T., and Wagner, N. J., *J. Catal.* **95,** 260 (1985).
17. Ko, E. I., Lester, J. E., and Marcelin, G., *ACS Symp. Ser.* **298,** 123 (1986).
18. Ruckenstein, E., and Hu, X. D., *J. Catal.* **100,** 1 (1986).
19. Wang, T., Lee, C., and Schmidt, L. D., *Surf. Sci.* **163,** 181 (1985).
20. Baker, R. T. K., Prestridge, E. B., and Garten, R. L., *J. Catal.* **56,** 390 (1979).
21. Weissman, J. G., Ko, E. I., and Wynblatt, P., *J. Vac. Sci. Technol. A* **5,** 1694 (1987).
22. Frondel, C., *in* "The System of Mineralogy," 7th ed., Vol. III (Silica Minerals). Wiley, New York, 1962.
23. Muilenberg, G. E. (Ed.), "Handbook of X-Ray Photoelectron Spectroscopy." Perkin–Elmer Corp., Eden Prairie, MN, 1979.
24. Grundner, M., and Halbritter, J., *J. Appl. Phys.* **51,** 397 (1980).
25. Grundner, M., and Halbritter, J., *Surf. Sci.* **136,** 144 (1984).
26. Schafer, H., Gruehn, R., and Schulte, F., *Angew. Chem. Int. Ed. Engl.* **5,** 40 (1966).
27. Burke, P. A., unpublished results.
28. Frevel, L. K., and Rinn, H. W., *Anal. Chem.* **27,** 1329 (1955).
29. Tamura, S., Kato, K., and Goto, M., *Z. Anorg. Allg. Chem.* **410,** 313 (1974).
30. Weissman, J. G., Burke, P. A., Wynblatt, P., and Ko, E. I., unpublished results.
31. Holtzberg, F., Reisman, A., Berry, M., and Berkenblit, M., *J. Amer. Chem. Soc.* **79,** 2039 (1957).
32. Terao, N., *J. Appl. Phys.* **4,** 8 (1965).
33. Norin, R., and Nolander, B., *Acta Chem. Scand.* **25,** 741 (1971).
34. Hibst, H., and Gruehn, R., *Z. Anorg. Allg. Chem.* **440,** 137 (1978).
35. Schafer, H., Schulte, F., and Gruehn, R., *Angew. Chem. Int. Ed. Engl.* **3,** 511 (1964).
36. Mertin, W., Andersson, S., and Gruehn, R., *J. Solid State Chem.* **1,** 419 (1970).
37. Waring, J. L., Roth, R. S., and Parker, H. S., *J. Res. Natl. Bur. Stand. Sect. A* **77,** 705 (1973).
38. Busca, G., Marchetti, L., Certi, G., and Trifiro, F., *J. Chem. Soc. Faraday Trans. 1* **81,** 1003 (1985).
39. Bond, G. C., and Bruckman, K., *Discuss. Faraday Soc.* **72,** 235 (1981).
40. Reddy, B. M., Chary, K. V. R., Rama Rao, B., Subrahmanyan, V. S., Sunandana, C. S., and Nag, N. K., *Polyhedron* **5,** 191 (1986).
41. Soled, S., Murrell, L. L., Wachs, I. E., McVicker, G. B., Sherman, L. G., Chan, S., Dispenziere, N. C., and Baker, R. T. K., *ACS Symp. Ser.* **279,** 165 (1985).
42. Hayden, T. F., and Dumesic, J. A., *J. Catal.* **103,** 366 (1987).
43. Bauer, E., and Poppa, H., *Thin Solid Films* **12,** 167 (1972).
44. Chen, M. C., *J. Electrochem. Soc.* **119,** 887 (1972).
45. Vossen, J. L., and O'Neill, J. J., *RCA Rev.* **29,** 149 (1968).
46. Iler, R. K., *in* "The Chemistry of Silica," Chapter 6. Wiley, New York, 1979.
47. Richter, M., Alsdorf, E., Fricke, R., Jancke, K., and Ohlmann, G., *Appl. Catal.* **24,** 117 (1986).
48. Bettman, M., and Yao, H. C., *in* "Sintering and Catalysis" (G. C. Kuczynski, Ed.), p. 165. Plenum, New York, 1975.
49. Fehlner, F. P., and Mott, N. F., *Oxid. Met.* **2,** 59 (1970).
50. Ibrahim, I., and Bright, N. F. H., *J. Amer. Ceram. Soc.* **45,** 221 (1962).
51. Izumi, F., and Kodama, H., *Z. Anorg. Allg. Chem.* **440,** 155 (1978).
52. Kato, K., and Tamura, S., *Acta Crystallogr. Sect. B* **31,** 673 (1975).
53. Gatehouse, B. M., and Wadsley, A. D., *Acta Crystallogr.* **17,** 1545 (1964).
54. Kato, K., *Acta Crystallogr. Sect. B* **32,** 764 (1976).